

Theoretical study on self-assembly in organic materials

Jianming CHEN¹, Qikai LI (✉)¹, Lingyi MENG¹ and Zhigang SHUAI (✉)^{1,2}

¹ Key Laboratory of Organic Solids, Beijing National Laboratory for Molecular Science (BNLMS), Institute of Chemistry, Chinese Academy of Sciences, Beijing 100190, China

² Department of Chemistry, Tsinghua University, Beijing 100084, China

Theoretical work related to the self-assembly of organic materials was dealt with, and the various mechanisms leading to self-assembly, such as transition metal mediated self-assembly, constraint induced self-assembly, covalent bond based self-assembly and *van der Waals* interaction driven self-assembly, etc., were discussed. The formation of ordered structures could be attributed to the competition between short range attractive forces and long-range repulsion, which was arising from dipole interaction or may result from a different mechanism based on a purely repulsive isotropic short-range pair potential with two characteristic length scales. Such mechanism could be exploited in the study of self-assembly process. First principles SAPT(DFT) interaction energy calculations, combined with the Williams-Stone-Misquitta method, offer the ability to improve the molecular dynamics (MD) accuracy which could in turn be used in the prediction of crystal structures and self-assembly tendency. The combination of experimental and theoretical studies could open new breakthroughs over the design, synthesis, and characterization of self-assembled materials.

Keywords self-assembly, theoretical study, mechanism, structure prediction

1 Introduction

Self-assembly is defined as the spontaneous formation of hierarchical structures generated from building blocks involving different energy (force) scales and multiple degrees of freedom. The self-assembly materials are created from specific strong exchange-correlation interactions between chemical particles (electrons, atoms, molecules and micro-crystals). Such interaction is distinguished from the well-known covalent, ionic and metal interparticle bonds [1]. Molecular self-assembly is a strategy for nanofabrication that involves the designation of molecules and supramolecular entities, which was caused to aggregate into desired structures by shape-complementarity. As a strategy, self-assembly has a number of advantages [2]: a) it carries out many of the most difficult steps in nanofabrication, involving atomic-level modification of structures using the very highly developed

techniques of synthetic chemistry; b) it draws from the enormous wealth of examples in nature for inspiration; self-assembly is one of the most important strategies used in biology for the development of complex functional structures; c) it can incorporate biological structures directly into the final systems as components; d) it tends to produce relatively defect-free and self-healing structures since it requires the target structures be the most thermodynamically stable ones open to the system. On the other hand, however, self-assembly also possesses a number of substantial intellectual challenges. Although there are countless examples of self-assembly all around us, the basic rules that govern these assemblies are not understood in detail, and self-assembling processes can not, in general, be designed and carried out according to our will. Many ideas that are crucial to the development of this area, such as the interplay between enthalpy and entropy, the nature of non-covalent forces that connect the particles in self-assembled molecular aggregates, etc., are simply not yet under our control. Therefore, the theoretical study on the deep underlying mechanisms for self-assembly is required.

As a new branch of chemistry, theoretical and computational chemistry has provided powerful theoretical support and scientific guide to the development of the whole chemistry. Especially, the rapid development of modern computer software and hardware technologies provide a solid foundation for the study of computational chemistry. The primary method of computational chemistry is the quantum mechanics method, which describes the behaviors of electrons in wave form that in turn are obtained by solving the Schrödinger equation. However, the quantum mechanics method is only applicable to simple molecules or systems of few electrons. More complex systems, for example, biomolecules, solvents or solid state systems, etc., are difficult to be handled directly. Therefore, researchers have resorted to classical mechanics to study the various complex systems and scored marvelous achievements; it gains further momentum with the development of modern computer hardware and software. To fully understand the mechanisms behind self-assembly, we need to resort to approaches in a multiscale way, i.e., from *ab initio* to the macroscopic scale. In this article, we are not trying to make it comprehensive, but rather to provide some illustrative examples intended to be used as a starting point for further studies.

2 Self-assembly in organic materials

Organic semiconductors have obtained great achievements for their extensive applications in organic light emitting display (OLED), organic field-effect transistor (OFET), solar cell electrodes and other nonlinear optical devices. Compared to inorganic semiconductors, organic materials have a lot of irreplaceable advantages, including low-cost, the convenience to synthesis, and light weight. Self-assembly provides an ideal way to fabricate different organic nanostructures. Using different synthetic schemes, experimentalists have successfully produced nanostructures with various kinds of morphologies.

Despite the great success in experimental research, the structure-property relationship is still an attracting topic for theoretical researchers. We could discover more potential application for different organic nanostructures if we knew the intrinsic interacting mechanisms of organic semiconductors. In recent years, the classical all-atom molecular dynamic (AA-MD) and coarse-grained molecular dynamic (CG-MD) simulations have been utilized in large self-assembling systems of hundred nanometers scale. With present processors, the CG model could handle systems containing ~1 million CG particles (~10 million atoms) and reach 100 ns in time scale [3]. The molecular dynamics (MD) models are also found to have great applications in biological systems as well

[4]. However, proper models for molecular simulation of organic material aggregation are still under development. The Monte Carlo (MC) modeling is another method to run simulations where conformational trajectory is changed by random transition instead of time step. Nevertheless, the MC simulation can use the force field scheme to describe the total energy of the system. These computational techniques are now used in various fields of research, such as carbon nanotubes channels [5–7], organic crystal packing, self-assembly monolayers (SAMs) [8–11], metal-organic frameworks (MOFs) [12–15], organoclay on inorganic crystalline [16–19], and colloidal nanoparticles aggregation [20,21]. The theoretical research on self-assembly mainly involves two factors, i.e., the driving interaction forces and spatial constraint. On one hand, there exists a principal driving force that leads the system to its final equilibrium self-assembly conformation. The driving force could be *van der Waals* interactions, hydrogen bonding, and covalent bonding etc. On the other hand, the substrates and templates could provide a steric constraint for the solvents or alkyl chains to form stable self-assembly architectures which are dependent on the shape of the substrates. In the following part of this section, works on self-assembly with different mechanisms will be discussed.

2.1 Transition metal mediated self-assembly

The structural and functional features of self-assembled supramolecular entities result from the information stored in their components and the components' intrinsic properties that are dictated by the presence of functional groups. A simple and general concept for generating ordered structures is based on the recognition-derived spontaneous assembly of complementary subunits. While organic systems are formed by many weak hydrogen bonds and *van der Waals* interactions, metal-ligand bonding interactions are much stronger and generally highly directional. As a result, due to various transition metal coordination geometries, metal complexes provide a pool of different acceptor subunits, which can be linked together by donor building blocks to form rigid frameworks. The final shape of self-assembled entity is not only defined through the metal coordination geometry, but also through the orientation of the interaction sites in a given ligand. The most common potential building units include nitrogen-containing heteroaryls, cyano-substituted aromatic ligands, *o*-catecholamides, hydroxamates, as well as phosphorus-containing ligands [22]. Self-assembly of pre-designed organic ligands with transition metal atoms is a powerful method for the construction of novel supramolecular architectures. For example, discrete 3D

molecules with very large (nanometer-order size) cavities can be prepared readily by multicomponent self-assembly through incorporating transition metal atoms [23].

Recently, continuous attention has been paid to the chirality of supramolecular systems [24], because of their important roles in both life and materials sciences [25]. In general, the chirality of supramolecules may be achieved by the following two strategies: a) at least one component is asymmetric or b) the interaction between achiral components is dissymmetrizing, and thus yielding a chiral association [26].

We have done some simulations on the achiral tripod-terpyridine, whose structure is shown in Figure 1. From the configuration, it is obvious that only one of the bonds around silica core is attached by a benzene cycle which results in the breaking up of symmetry. The most preferred growing direction would be along or close to the benzene plane. The MD simulations indicate that two neighboring terpyridine molecules tend to form a subunit by two biting jaws, which would be perpendicular to each other without silver ions. However, the introductions of silver ions fix the neighboring terpyridine planes in a tilt degree and make the plane deviate from perpendicularity to a lower-energy conformation [27]. The MD results showed that the tripod terpyridine tends to grow in a spiraling style with the addition of silver ions, which leads the aggregation to a helical arrangement. Due to the compression between ligands and Ag cations, these intermediate flat strips can further twist and roll into helical structures. In the case of lower concentrations of Ag cations,

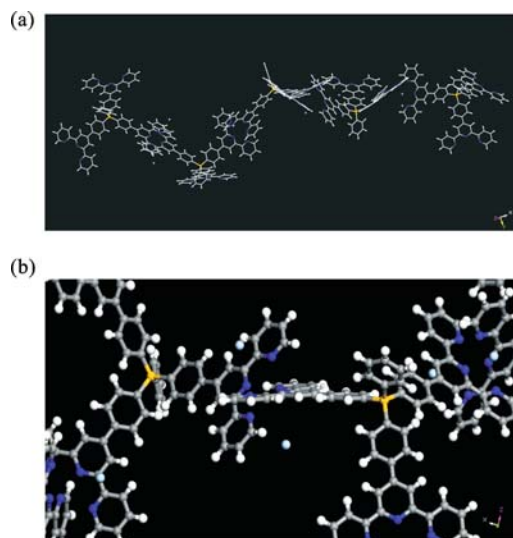


Figure 1 View of the achiral tripod-terpyridine. (a) Typical configuration. (b) One of enlarged typical coordination arrangements between two terpyridines and Ag cations. Yellow spheres stand for Si atoms, cyan spheres for silver ions. Blue lines represent terpyridine parts.

decreased steric controllability results in the formation of twisted fibrils.

In recent years chemists have made great efforts on using transition metal complexes for bridging bidentate ligands to construct predictable, multi-dimensional infinite networks. The advances made in this field have shown how ligand design and the properties of the transition metal and counter-anion can be used to control the network geometry and hence the crystal structure [28]. A variety of transition metal based supramolecular systems can be carefully designed to perform a desired function such as molecular sensing and photo-switching [29].

2.2 Constraint induced self-assembly

The nano-sized materials constitute key elements of advanced functional devices due to their size-sensitive electrical, optical, magnetic and chemical properties. To integrate nano-structures into real devices, it is desirable to form them with controlled size and distribution on substrates compatible with current fabrication technologies. By using physical templates to alter the surface environment, the self-forming and self-ordering processes can be initiated in material systems that have limited or no inherent order. The key to the templating of the self-assembling systems is an understanding of the response of the system when its equilibrium period is incommensurate with the dimensions of the guiding template. For example, in the very thin carbon nanotubes, the water molecules could form the so-called quasi one-dimensional (Q1D) structures that might constitute a new phases of ice, different from the 15 polymorphic phases of bulk ice identified experimentally thus far [30,31]. Our simulations [6] showed that, in the case of (8, 8) and (9, 9) single-walled nanotubes (SWNTs), the Q1D n-gonal structures can be formed due to the nano-constraint effect of carbon nanotube. The more orderly 6-gonal lattice is found in case of the (9, 9) single-walled nanotube, as shown in Figure 2.

The two-dimensional (2D) self-assembled structures induced by steric constraint are widely reported for their

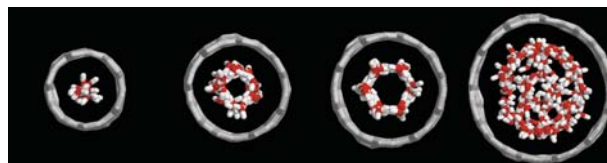


Figure 2 Self-assembling structures (top view) of water molecules confined by one-dimensional channels. From left to right figures are for water inside (6, 6), (8, 8), (9, 9), and (12, 12) carbon nanotubes. The red spheres represent oxygen atoms and white spheres represent hydrogen atoms.

potential application in molecular electronics. We have done some simulations on the self-assembling system formed by α -phthalocyanine (α -H₂Pc) and p-sexiphenyl (p-6P). The three initial assembling membrane models have been established to run the MD simulation [32]. The optimized conformation with the lowest energy was obtained after 100 ps relaxation as shown in Figure 3. The dihedral angle between α -H₂Pc (010) and p-6P (010) surface is about 9°. These calculations are in good agreement with Yang's experimental work [33].

2.3 Covalent bond based self-assembly

The interface of self-assembled monolayers (SAMs) exhibits excellent adsorption capabilities for technological and biological applications. In the recent decades, investigation of interfacial properties has been an interesting topic in surface chemistry. SAMs with different features were fabricated and characterized in experiments [34,35]. Gold, silver, and copper are used as substrates for most SAMs. Alkanethiols terminated by functional groups [–CH₃, –OH, –COOH or oligo (ethylene glycol) (OEG)] can be self-organized into highly ordered structure on specific substrate surface. As the sulfur-metallic bonding is the covalent strong bonding, SAMs are in relatively high stability. Because of the special surface features and stability, SAMs have potential applications in chemical and biological sensors and molecular

electronics. The structural properties of SAMs are determined by the substrate-headgroup interactions and chain-chain interactions, as shown in Figure 4. Understanding the intrinsic structure-property relationship of SAMs is a very important task for functional materials design.

The MD simulations revealed that the conformation of SAMs is closely related to the packing density, chain length, and temperature [36,37]. Additionally, MD simulation has become the most common computational technique for the research of surface features. SAMs exhibit water-confinement effects due to the terminated group which determines whether the SAM is hydrophobic or hydrophilic. In order to study water-confinement effect of SAMs, molecular-level simulations on water-SAM systems have been carried out [38]. In addition, comparison between hydrophobic and hydrophilic surfaces has also been reported. Jensen et al. [39] investigated water confinement on crystalline surfaces of hydrophobic *n*-alkane C₃₆H₇₄ and hydrophilic *n*-alcohol C₃₅H₇₁OH using MD simulations. Results showed that the water orientations are different at the two surfaces. The water molecules at hydrophobic surface show the characteristic diffusive behavior and orientation ordering due to the lack of hydrogen bonding with the surface. Furthermore, the MD simulations have widened the application in the research of protein adsorption [40,41], oxygen transportation [42], phase separation [43] on SAMs, and have already provided very promising results.

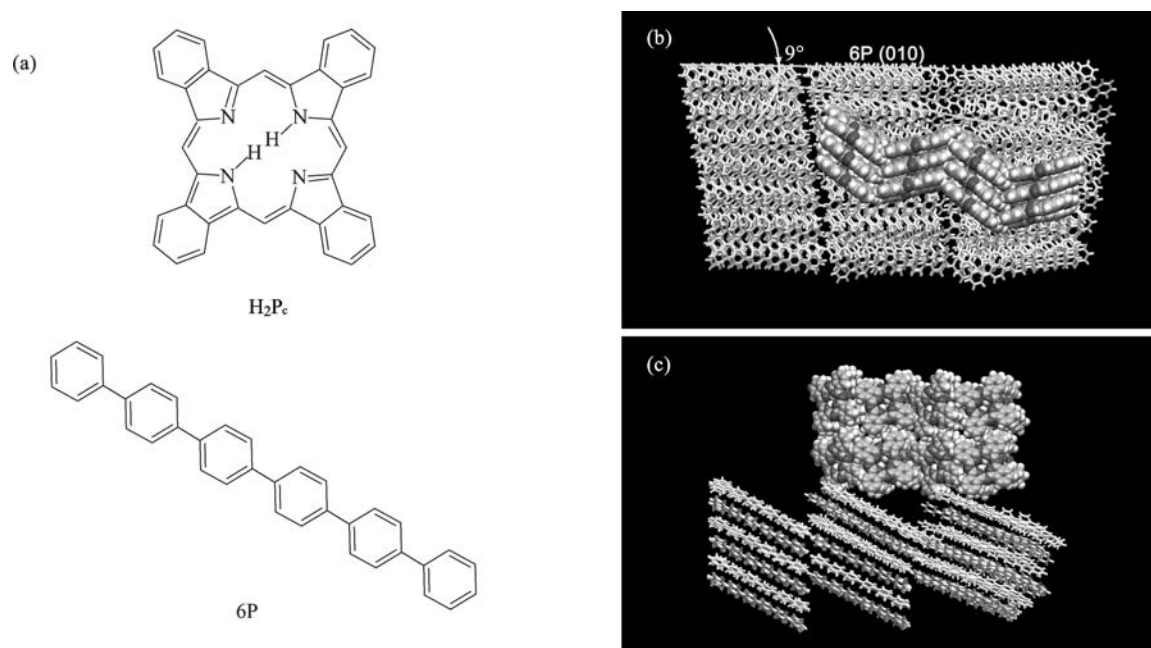


Figure 3 The MD results of the assembled model in its stable configuration. (a) The molecular structures of H₂Pc and 6P; (b) top view and (c) side view of the simulated final conformation of the 2D self-assembling system formed by H₂Pc and 6P. In the model, the white frame represents 6P molecules; the green (C), blue (N) and white (H) spheres represent the H₂Pc molecules.

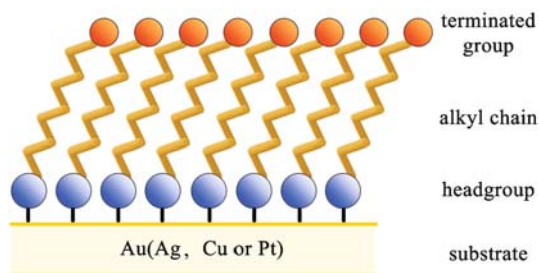


Figure 4 Typical structure of the SAMs. The substrate surface is usually Au(111), Ag(111), and Cu(111). Thiol headgroup –SH can form covalent bond with metal atoms.

2.4 van der Waals interaction driven self-assembly

Organic surfactants have been used to modify silicate surface. For the last few years, organic-inorganic complexes have attracted much attention for its potential mechanic application in materials science. Unlike SAMs, the structures of organic-inorganic complexes are dependent on non-covalent bonding. By intermolecular van der Waals interactions, Coulombic interactions and hydrogen bond interactions, silicates, such as montmorillonite, mica, graphite and pyrophyllite, can interact with long-chain hydrocarbon to form an improved complex. The obtained organic-inorganic complexes exhibit excellent properties on the aspects of mechanic strength, heat stability, selective adsorption, and cationic exchange capability. Experiments have provided various methods to characterize the conformation of the complex. Conformation change should be related to the chain length, side group, and experimental conditions (temperature, pressure, etc.) Theoretical tools can be a convenient scheme to study dynamic behaviors and capacities of different complexes [44].

Enevoldsen et al. [45,46] have done some researches on the side chain effect in organic-inorganic complexes. A theoretical study on the two alkyl molecules adsorbed onto graphite was also reported. Both adsorbates, *n*-alkane $C_{24}H_{50}$ and branched $C_{30}H_{62}$, have C_{24} backbone. The MD simulations indicated that, parts of side groups in $C_{30}H_{62}$ change from *gauche* conformation to *trans* conformation. The order decreases when side groups exist.

Zeng et al. [47] investigated the layering behaviors and interlayer structures of organo-montmorillonite complexes. Several alkylammoniums with different alkyl chain length were modeled as adsorbates moving on the static montmorillonite clay. The clay structures included monolayers, bilayers, pseudo-trilayers and paraffin-type layers. Simulations were performed to predict interlayer densities and cation exchange capabilities. It was found that two alkyl chains lied flat on the clay surface, and the quasi-quadrilayers were observed due to the double alkyl chain modification. In some

conditions, alkyl chains form into interlace and jump to the next nearest layer. These interesting results provide guidance of organoclay fabrication.

Conjugated organic oligomers can form relatively more stable self-assembled membrane architectures due to intermolecular and intramolecular π - π stacking interaction. For example, β -alkylated oligothiophenes monolayers on graphite substrate have been investigated by Gus'kova et al. [48]. By comparing the MD results, they found that monolayers formed by $C_{12}H_{25}$ substituted oligothiophene exhibit higher degree of order when stacking. In addition, the nearest neighboring interactions also have some contributions to membrane fabrication.

Up to now, direct modeling of self-assembly and prediction of self-assembly tendency are still having a long way to go. Possibly the many-body effects and other unidentified factors are having their role in the self-assembling process which will be partially dealt with in the following sections.

3 Forces in play behind self-assembly

The theoretical development in the field of self-organizing materials is based on the balance between the chemical forces and some effects of thermal, mechanical, and electromagnetic fluctuations. Theoretical researches revealed that the stripe formation can be attributed to the competition between short range attractive forces and long-range repulsion arising from dipole interaction [49]; or it may result from a different mechanism based on a purely repulsive isotropic short-range pair potential with two characteristic length scales [50]. The above-mentioned picture can clearly be demonstrated by the magnetic domain formation. Since it costs energy to make a domain wall, one might wonder why more than one domain ever forms in the first place. The reason is that the formation of domains saves energy associated with dipolar fields. This dipolar energy can be saved by breaking the sample into domains, but each created domain costs energy because of the cost of the domain walls. Therefore, in the same way as the size of a domain wall is a balance between the exchange and anisotropy energies, the formation of domains is a balance between the cost of a demagnetizing field and the cost of a domain wall. This revealed that the competition of more than one type of energy triggers the domain formation.

However, domain formation can occur even when there is only one force. The MD simulation of isotropic particles has been carried out by using Malescio's force model [50]. Only repulsive interactions are considered in this model. Stripe domain pattern can also be obtained by resorting to MD simulations, as shown in Figure 5. Therefore, it could be concluded that the competition-free stripe domains could be fabricated in bulk systems.

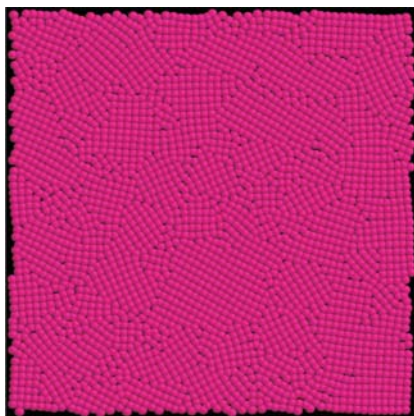


Figure 5 Polycrystal morphology of particles obtained by MD simulation.

It has been well recognized that phase separation on molecular scale is caused by the interaction energy between neighboring molecules, as is known from the van der Waals equation [51]. When the interaction energy between hetero-species is predominant compared to that between homo-species, a phase separation is likely to occur. A quantitative approach of phase separation has been described by the two- or three-dimensional Ising model of spins in which phases are formed at a temperature lower than a critical temperature [52]. In this regard, more theoretical work needs to be performed.

4 Theoretical prediction of crystal structure

In the nanoscience and nanotechnology field, the extremely important challenges are how to exploit synthetic methods for structures regulated at atomic scale and to construct materials across the hierarchy of length scales from the atomistic to the mesoscopic and/or the macroscopic scale. The nanosize building blocks with low dimensionality, such as nanowires, nanorods, nanotubes, and nanosheets, have emerged as technically important systems, which facilitate us to investigate the influence of size and dimensionality on their optical, magnetic and electronic properties as well as potential components for nanodevices. Because of low dimensionality and small scale, the existing theories may no longer valid, thus new theories are needed. On the other hand, because of the reduced dimensional scale, the theoretical work could be more appropriate to be carried out.

At present, the theoretical studies on self-assembly in organic materials is lagging far behind the experiments. As a result, much more efforts are required in theoretical aspects to answer the following fundamental questions [1].

- structures and phases that can be formed;
- parameters that control assembling and growth;
- parameters defining the order;

- kinetics and thermodynamics of phase transitions;
- influence of the chemistry, shapes, and dimensions of the building blocks;
- driving forces and kinetics of self-assembly processes.

The prediction of crystal structures of organic molecules constitutes one of the grand challenges of computational chemistry [53,54]. As a first step, herein we introduce a method dubbed as SAPT(DFT) [55–59] which could be used to predict the crystal structures for small molecules. SAPT stands for symmetry-adapted perturbation theory while DFT for density function theory. This is in turn attributed to the significant developments in deriving intermolecular forces from electronic structure theory, namely, the SAPT(DFT) method for the calculation of interaction energies of dimers and the Williams–Stone–Misquitta distribution technique for obtaining distributed polarizabilities and dispersion coefficients. These methods can be combined together to obtain the analytic atom-atom potential in a numerically robust and straightforward manner.

The SAPT(DFT) is a model for describing the intermolecular interaction, which combines SAPT and DFT and modifies the inaccurate XC function. As a result, more reliable results are obtained. In SAPT theory, the Hamiltonian of the dimer is partitioned as:

$$H = F + \xi W + \lambda V,$$

where $F = F_A + F_B$ is the sum of the Fock operators for monomers A and B, respectively, $W = W_A + W_B$ is the sum of the Møller–Plesset fluctuation operators for the monomers, and $V = H - H_A - H_B$ is the intermolecular interaction operator. Williams and Chabalowski included only terms of zeroth order in ξ , effectively neglecting the second operator and using the simplified Hamiltonian:

$$H = F + \lambda V,$$

which may be regarded as the Hamiltonian of two interacting “Kohn–Sham molecules”. In accordance with the perturbation theory, we expand the energy up to the second order:

$$E_{\text{int}}^{\text{SAPT(KS)}} = E_{\text{elst}}^{(1)}(\text{KS}) + E_{\text{exch}}^{(1)}(\text{KS}) + E_{\text{ind}}^{(2)}(\text{KS}) \\ + E_{\text{exch-ind}}^{(2)}(\text{KS}) + E_{\text{disp}}^{(2)}(\text{KS}) + E_{\text{exch-disp}}^{(2)}(\text{KS})$$

Here, $E_{\text{elst}}^{(1)}(\text{KS})$ and $E_{\text{exch}}^{(1)}(\text{KS})$ are the first-order electrostatic and exchange-repulsion energies, $E_{\text{ind}}^{(2)}(\text{KS})$ and $E_{\text{exch-ind}}^{(2)}(\text{KS})$ are the second-order induction and exchange-induction energies, $E_{\text{disp}}^{(2)}(\text{KS})$ and $E_{\text{exch-disp}}^{(2)}(\text{KS})$ are the second-order dispersion and exchange-dispersion energies. The higher order terms are not expected to be significant for systems without hydrogen bonds and can therefore be neglected. $E_{\text{elst}}^{(1)}(\text{KS})$ represents the Coulomb interaction between two

unperturbed monomer charge distributions:

$$E_{\text{elst}}^{(1)} = \int \frac{\rho^{\text{A}}(\mathbf{r}_1)\rho^{\text{B}}(\mathbf{r}_2)}{|\mathbf{r}_1 - \mathbf{r}_2|} d^3\mathbf{r}_1 d^3\mathbf{r}_2.$$

In SAPT(DFT), the total charge densities that appear in this expression are evaluated using Kohn–Sham DFT. $E_{\text{exch}}^{(1)}$ (KS) represents the main exchange contribution to the interaction energy, an accurate evaluation of $E_{\text{exch}}^{(1)}$ (KS) is difficult; it can only be obtained numerically.

The induction energy plays an important role in determining the structures of polar molecules clusters. The cooperative nature of the induction means that, for polar molecules, induction effects dominate the many-body contributions to the interaction energy. These many-body effects can be very important in determining the structures of clusters of molecules. However, this interaction energy component is often neglected or treated incorrectly [59]. This is not only due to the difficulty to calculate accurately, but also because important aspects of the induction energy are still poorly understood. First, it is not pair-additive. Second, it is cooperative. The most general way to calculate the induction is to use the frequency-dependent density susceptibility (FDDS), $R(\mathbf{r}, \mathbf{r}' | \omega)$ describes the change in charge density at \mathbf{r} due to a delta-function change in electrostatic potential at \mathbf{r}' oscillating at frequency ω . To describe induction we only need the static FDDS, $R(\mathbf{r}, \mathbf{r}' | 0)$; it can be calculated efficiently and accurately by modern methods. As a result, $E_{\text{ind}}^{(2)}$ (X) can be rewritten in terms of FDDS function $\alpha_X(\mathbf{r}, \mathbf{r}' | \omega)$ evaluated at zero frequency [60]:

$$E_{\text{ind}}^{(2)}(X) = -\frac{1}{2} \iint \alpha_X(\mathbf{r}, \mathbf{r}' | 0) \hat{\omega}(\mathbf{r}) \hat{\omega}(\mathbf{r}') d\mathbf{r} d\mathbf{r}',$$

where

$$\alpha_X(\mathbf{r}, \mathbf{r}' | \omega) = 2 \sum_{k \neq 0} \frac{E_k^X - E_0^X}{(E_k^X - E_0^X)^2 - \omega^2} \cdot \langle \Phi_0^X | \hat{\rho}_X(\mathbf{r}) | \Phi_k^X \rangle \times \langle \Phi_k^X | \hat{\rho}_X(\mathbf{r}') | \Phi_0^X \rangle.$$

$E_{\text{disp}}^{(2)}$ (KS) originates from instantaneous interaction of electrical multipole moments, the expression for the dispersion energy in terms of FDDSs can be expressed as:

$$E_{\text{disp}}^{(2)} = -\frac{1}{2\pi} \int_0^\infty \iint \alpha_{\text{A}}(\mathbf{r}_1, \mathbf{r}'_1 | i\omega) \cdot \alpha_{\text{B}}(\mathbf{r}_2, \mathbf{r}'_2 | i\omega) \times \frac{d\mathbf{r}_1 d\mathbf{r}_2 d\mathbf{r}'_1 d\mathbf{r}'_2}{|\mathbf{r}_1 - \mathbf{r}_2| |\mathbf{r}'_1 - \mathbf{r}'_2|} d\omega.$$

$E_{\text{exch-ind}}^{(2)}$ (KS) and $E_{\text{exch-disp}}^{(2)}$ (KS) are used to describe the second-order electronic exchange-correlation energy, including coupling to the induction energy and the dispersion

energy. Compared with $E_{\text{exch}}^{(1)}$ (KS), the second-order exchange-correlation energy occupies a much smaller portion in the total energy. However, when calculating the interaction potential of dimer, the second-order energy has significant influence on the accuracy of results.

The SAPT(DFT) includes the electronic correlation and can normally yield more accurate results. Misquitta et al. have applied the SAPT(DFT) algorithm to dimers such as He₂, Ne₂, (H₂O)₂, and (CO₂)₂. The calculated results are in perfect agreement with experimental standard values [59,60]. Later on, by using the aug-cc-pVTZ base sets, they computed the dimer interaction potentials for small organic molecules such as formamide, N-methyl propanamide, benzene, and 3-azabicyclo[3.3.1]nonane-2,4-dione. The results are quite satisfactory. In addition, Misquitta et al. have also used the SAPT(DFT) theory to predict the crystal structure of C₆Br₂ClFH₂ [61], the deviations of the crystal structure parameters a , b and c are -0.09 , 0.28 , 0.10 Å from experimental results, respectively. This is a great achievement. These results all prove that the potential described by the SAPT(DFT) theory is closer to the real potential.

When using MD simulation to study the self-assembly of nanostructure, an appropriate force field is needed to describe the non-bonded interaction potential. The intermolecular interaction potential has always been the bottleneck to development of DFT theory. However, the SAPT(DFT) theory offers the ability to improve the MD accuracy from the quantum mechanics point of view. When doing self-assembly simulation with MD simulations, we first resort to the SAPT(DFT) to calculate the molecular dimer structure, and then obtain a basic unit cell configuration. Later on, by repeating the unit cell, we obtain the supercell of the cluster. The whole process is shown in Figure 6. Here the Sobol sequence is used since it can better fill up a hypercube than the standard MC method. Price and Misquitta et al. have successfully used a first principle method in predicting the crystal structure [61].

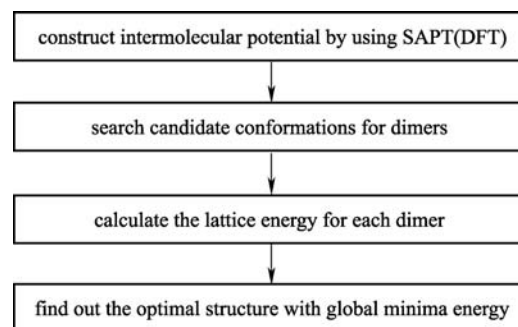


Figure 6 Crystal structure prediction by using SAPT(DFT).

The molecular force field is used to describe the interaction among the unit cells. In this way, by combining the SAPT (DFT) theory and the force field method with MD simulations, we may be able to better obtain the structure information of nanoscale clusters and improve the structure predication capability of MD simulations.

5 Conclusions and prospects

Many of the current synthetic methodologies have their origins from traditional solid state chemistry, while extra efforts have been placed on the precise control of the size and shape of the nanomaterials. The level of control, however, is far from perfect at the present stage. Significant effort should be placed on the monodispersity control of the nanoscale building blocks.

In many functional architectures in nature, the complex superstructure is the result of the self-assembly and self-organization of smaller building blocks [62]. Chemists have been attempting to fabricate functional devices from simple molecular components that are programmed to self-organize into hierarchical structures in an analogous fashion to biological systems [63]. To succeed in this goal, it is very important to have control over the self-organization process at different hierarchical levels. First, the constituting molecules with desired (photo)catalytic, electronic, magnetic or optical properties must be equipped with handles for intermolecular recognition [64,65]. Second, the building blocks need to self-assembled into larger structures with a predictable morphology. Third, it is a challenge to control the self-organization of these self-assembled supermolecules into functional nanoarchitectures. Finally, the collection of these structures should result in a functional device or material [66,67].

The idea behind the current nanotechnology is to reproduce what nature already does: to generate materials atom-by-atom and/or molecule-by-molecule. That is a bottom-up approach. This will not only allow researchers to tune functional/structural properties, but might also be possible for them to design intelligent advanced materials. To achieve this goal, new synthesis methods allowing structural organization from the dimensions of molecules to the sizes of macroscopic objects must be developed, together with new characterization methods to understand the structure and the potential of self-assembled materials [68]. Experiments coupled with theoretical studies could open new breakthroughs over the design, synthesis, and characterization of self-assembled materials.

Acknowledgements This work was supported by the National Natural Science Foundation of China (Grant Nos. 10425420 and 20773145), the Ministry of Science and Technology of China (Grant

Nos. 2006CB806200 and 2006CB932100), as well as the Chinese Academy of Sciences including its CNIC supercomputer center.

References

1. Depero, L. E.; Lucia, C. M., *Curr. Opin. Solid State Mater. Sci.* **2004**, *8*, 103–109
2. Whitesides, G. M., *Self assembly and nanotechnology, in The fourth foresight conference on molecular nanotechnology*; CA, USA, **1995**
3. Klein, M. L.; Shinoda, W., *Science* **2008**, *321*, 798–800
4. Van Gunsteren, W. F.; Bakowies, D.; Baron, R.; Chandrasekhar, I.; Christen, M.; Daura, X.; Gee, P.; Geerke, D. P.; Glättli, A.; Hünenberger, P. H.; Kastenholz, M. A.; Ostenbrink, C.; Schenk, M.; Trzesniak, D.; Yu, H. B., *Angew. Chem.* **2006**, *45*, 4064–4092
5. Dong, K.; Zhou, G. H.; Liu, X. M.; Yao, X. Q.; Zhang, S. J.; Lyubartsev, A., *J. Phys. Chem. C* **2009**, *113*, 10013–10020
6. Meng, L.; Li, Q.; Shuai, Z., *J. Chem. Phys.* **2008**, *128*, 134703–7
7. Meng, L.; Li, Q.; Shuai, Z., *Sci. China Ser. B Chem.* **2009**, *52*, 137–143
8. Ismail, A. E.; Grest, G. S.; Stevens, M. J., *Langmuir* **2007**, *23*, 8508–8514
9. Lane, J. M. D.; Chandross, M.; Stevens, M. J.; Grest, G. S., *Langmuir* **2008**, *24*, 5209–5212
10. Raut, V. P.; Agashe, M. A.; Stuart, S. J.; Latour, R. A., *Langmuir* **2005**, *21*, 1629–1639
11. Mar, W.; Klein, M. L., *Langmuir* **1994**, *10*, 188–196
12. Dubbeldam, D.; Walton, K. S.; Ellis, D. E.; Snurr, R. Q., *Angew. Chem. Int. Ed.* **2007**, *46*, 4496–4499
13. Han, S. S.; Mendoza-Cortés, J. L.; Goddard, W. A. III, *Chem. Soc. Rev.* **2009**, *38*, 1460–1476
14. Rosenbach, N. Jr; Jobic, H.; Ghoufi, A.; Salles, F.; Maurin, G.; Bourrelly, S.; Llewellyn, P. L.; Devic, T.; Serre, C.; Férey, G., *Angew. Chem. Int. Ed.* **2008**, *47*, 6611–6615
15. Zhou, W.; Wu, H.; Yildirim, T.; Simpson, J. R.; Hight Walker, A. R., *Phys. Rev. B* **2008**, *78*, 054114–5
16. Gardebien, F.; Gaudel-Siri, A.; Bredas, J. L.; Lazzaroni, R., *J. Phys. Chem. B* **2004**, *108*, 10678–10686
17. Gesquiere, A.; Abdel-Mottaleb, M. M. S.; De Feyter, S., De Schryver, F. C.; Schoonbeek, F.; van Esch, J.; Kellogg, R. M.; Feringa, B. L.; et al, *Langmuir*, **2000**, *16*, 10385–10391
18. He, H.; Galy, J.; Gerard, J. F., *J. Phys. Chem. B* **2005**, *109*, 13301–13306
19. Heinz, H.; Castelijns, H. J.; Suter, U. W., *J. Am. Chem. Soc.* **2003**, *125*, 9500–9510
20. Beznosyuk, S. A.; Lerh, Y. V.; Zhukovsky, T. M.; Zhukovsky, M. S., *Mater. Sci. Eng. C* **2009**, *29*, 884–888
21. Striolo, A., *Nanotech.* **2008**, *19*, 445606
22. Leininger, S.; Olenyuk, B.; Stang, P. J., *Chem. Rev.* **2000**, *100*, 853–908
23. Müller, I. M.; Robson, R.; Separovic, F., *Angew. Chem. Int. Ed.* **2001**, *40*, 4385–4386

24. Jeong, K. S.; Kim, S. Y.; Shin, U. S.; Kogej, M.; Hai, N. T.; Broekmann, P.; Jeong, N.; Kirchner, B.; et al, *J. Am. Chem. Soc.* **2005**, *127*, 17672–17685
25. Chen, C. L.; Kang, B. S.; Su, C. Y., *Aust. J. Chem.* **2006**, *59*, 3–18
26. Suárez, M.; Branda, N.; Lehn, J. M.; Decian, A.; Fischer, J., *Helv. Chim. Acta* **1998**, *81*, 1–13
27. He, X. R.; Li, Q. K.; Li, Y. L.; Wang, N.; Song, Y. B.; Liu, X. F.; Yuan, M. J.; Xu, W.; et al, *J. Phys. Chem. B* **2007**, *111*, 8063–8068
28. Blake, A. J.; Champness, N. R.; Hubberstey, P.; Li, W. S.; Withersby, M. A.; Schroder, M., *Coord. Chem. Rev.* **1999**, *183*, 117–138
29. Sun, S. S.; Lees, A. J., *Coord. Chem. Rev.* **2002**, *230*, 170–191
30. Lobban, C.; Finney, J. L.; Kuhs, W. F., *J. Chem. Phys.* **2000**, *112*, 7169–7180
31. Salzmann, C. G.; Radaelli, P. G.; Hallbrucker, A.; Mayer, E.; Finney, J. L., *Science* **2006**, *311*, 1758–1761
32. Chen, J. M.; Meng, L. Y.; Li, Q. K.; Shuai, Z. G., *Molecular dynamic simulation on self-assembling system formed by α -phthalocyanine and p-sexiphenyl*, in *The 8th International Conference on Optical Probes of Conjugated Polymers and Organic Nanostructures*; Beijing, China, 2009; p 84
33. Yang, J.; Wang, T.; Wang, H.; Zhu, F.; Li, G.; Yan, D., *J. Phys. Chem. B*, **2008**, *112*, 3132–3137
34. Ulman, A., *Chem. Rev.* **1996**, *96*, 1533–1554
35. Love, J. C.; Estroff, L. A.; Kriebel, J. K.; Nuzzo, R. G.; Whitesides, G. M., *Chem. Rev.* **2005**, *105*, 1103–1170
36. Rai, B.; Sathish, P.; Malhotra, C. P.; Pradip; Ayappa, K. G., *Langmuir* **2004**, *20*, 3138–3144
37. Vaia, R. A.; Teukolsky, R. K.; Giannelis, E. P., *Chem. Mater.* **1994**, *6*, 1017–1022
38. Stevens, M. J.; Grest, G. S., *Biointerphases*, **2008**, *3*, FC13–FC22
39. Jensen, M. O.; Mouritsen, O. G.; Peters, G. H., *J. Chem. Phys.* **2004**, *120*, 9729–9744
40. Zheng, J.; Li, L.; Chen, S.; Jiang, S., *Langmuir* **2004**, *20*, 8931–8938
41. Zheng, J.; Li, L.; Tsao H. K.; Sheng, Y. J.; Chen, S.; Jiang, S., *Biophys. J.* **2005**, *89*, 158–166
42. Srivastava, P.; Chapman, W. G.; Laibinis, P. E., *Langmuir* **2009**, *25*, 2689–2695
43. Shevade, A.V.; Zhou, J.; Zin, M. T.; Jiang, S., *Langmuir* **2001**, *17*, 7566–7572
44. Heinz, H.; Vaia, R. A.; Krishnamoorti, R.; Farmer, B. L., *Chem. Mater.* **2007**, *19*, 59–68
45. Enevoldsen, A. D.; Hansen, F. Y.; Diama, A.; Criswell, L.; Taub, H., *J. Chem. Phys.* **2007**, *126*, 104703–10
46. Enevoldsen, A. D.; Hansen, F. Y.; Diama, A.; Taub, H.; Dimeo, R. M.; Neumann, D. A.; Copley, J. R. D., *J. Chem. Phys.* **2007**, *126*, 104704–17
47. Zeng, Q. H.; Yu, A. B.; Lu, G. Q.; Standish, R. K., *Chem. Mater.* **2003**, *15*, 4732–4738
48. Gus'kova, O. A.; Mena-Osteritz, E.; Schillinger, E.; Khalatur, P. G.; Bäuerle, P.; Khokhlov, A. R., *J. Phys. Chem. C* **2007**, *111*, 7165–7174
49. Aoki, K., *J. Electroanal. Chem.* **2001**, *513*, 1–7
50. Malescio, G.; Pellicane, G., *Nat. Mater.* **2003**, *2*, 97–100
51. Rowlinson, J. S.; Widom, B., *Molecular Theory of Capillarity*; Oxford University Press: Oxford, 1989; p 50–68
52. Wannier, G. H., *Statistical Physics*; Dover Publications, 1987
53. Dunitz, J. D., *Chem. Comm.* **2003**, 545–548
54. Dunitz, J. D.; Scheraga, H. A., *Proc. Nat. Acad. Sci. U. S. A.* **2004**, *101*, 14309–14311
55. Heßelmann, A.; Jansen, G., *Chem. Phys. Lett.* **2002**, *362*, 319–325
56. Heßelmann, A.; Jansen, G.; Schutz, M., *J. Chem. Phys.* **2005**, *122*, 014103–17
57. Misquitta, A. J.; Jeziorski, B.; Szalewicz, K., *Phys. Rev. Lett.* **2003**, *91*, 033201
58. Misquitta, A. J.; Szalewicz, K., *Chem. Phys. Lett.* **2002**, *357*, 301–306
59. Misquitta, A. J.; Szalewicz, K., *J. Chem. Phys.* **2005**, *122*, 214109–19
60. Misquitta, A. J.; Podeszwa, R.; Jeziorski, B.; Szalewicz, K., *J. Chem. Phys.* **2005**, *123*, 214103–14
61. Misquitta, A. J.; Welch, G.W. A.; Stone, A.J.; Price, S. L., *Chem. Phys. Lett.* **2008**, *456*, 105–109
62. Choi, I. S.; Bowden, N.; Whitesides, G. M., *Angew. Chem. Int. Ed.* **1999**, *38*, 3078–3081
63. Drain, C. M., *Proc. Nat. Acad. Sci. U. S. A.* **2002**, *99*, 5178–5182
64. Hecht, S., *Angew. Chem. Int. Ed.*, **2003**, *42*, 24–26
65. Lehn, J. M., *Supramolecular Chemistry*; Wiley-VCH: Weinheim, 1995
66. Elemans, J. A. A. W.; Rowan, A. E.; Nolte, R. J. M., *J. Mater. Chem.* **2003**, *13*, 2661–2670
67. Lehn, J. M., *Science* **2002**, *295*, 2400–2403
68. Cava, R. J.; DiSalvo, F. J.; Brus, L. E.; Dunbar, K. R.; Gorman, C. B.; Haile, S. M.; Interrante, L. V.; Musfeldt, J. L.; et al, *Prog. Solid State Chem.* **2002**, *30*, 1–101